Available online at www.sciencedirect.com
ScienceDirect
Journal of the European Ceramic Society 29 (2009) 2527–2535
www.elsevier.com/locate/jeurceramsoc

Studies on a novel bioactive glass and composite coating with hydroxyapatite on titanium based alloys: Effect of γ-sterilization on coating

Sanghamitra Bharati, Chidambaram Soundrapandian, Debabrata Basu, Someswar Datta *

Bioceramic & Coating Division, Central Glass & Ceramic Research Institute, Kolkata 70032, India

Received 12 August 2008; received in revised form 9 February 2009; accepted 23 February 2009
Available online 25 March 2009

Abstract

A novel silicate based bioactive glass coating composition containing B_2O_3 and TiO_2 having matching thermal properties with that of Ti_6Al_4 V implants was developed and characterized. A conventional vitreous enamelling technique was used for coating small flat surface and curved surface of small rods. Hydroxyapatite (HAp) micro and nano-crystalline particles were used to prepare bioactive glass-HAp composite coating. Scratch testing was used to study the coating adhesion and its fracture behaviour under simulated conditions. As observed from scratch testing results, adhesion strength of the coating improved from 21 N normal load to 27 N and 32 N on addition of micro-HAp and nano HAp powder, respectively, to bioactive glass matrix. Further, sterilization of the coated samples with 25 kGy gamma irradiation substantially enhanced the adhesion of glass coating and HAp-composite coating.

Keywords: Composites; Glass; Apatite; Biomedical applications; Mechanical properties

1. Introduction

Metallic implants (stainless steel, titanium and its alloy (Ti_6Al_4 V) are widely used as load bearing orthopaedic, dental implants and plastic surgery. However, being bio-inert, they suffer from unfavourable bioactive fixation with the surrounding hard tissues[1,2] which limits their effective service life. Therefore, they are often coated with other bioactive materials such as hydroxyapatite (HAp), bioactive glass, etc. by various techniques to enable cementless fixation and to improve their integration to the adjacent hard or soft tissues.[3–9]

It has been established that bioactive glasses in SiO_2–Na_2O–CaO–P_2O_5 system have higher bioactivity in comparison to hydroxyapatite[10] and consequently the material has become a natural choice to be used as a coating on metallic implants. Reports of Tomsia and co-workers[6–8] to develop bioactive glass coated implants of titanium alloys was a failure as the thermal expansion mismatch between the glass and the substrate generated thermal stresses which after heat treatment resulted interfacial cracks that propagated during actual use and eventually led to failure of the coating. The most important design factors for the successful development of new bioactive glass coating for load bearing implants are (1) the coating application technique should not alter the properties of the metal and the coating material, (2) the coating should have chemically bonded interface with optimum adhesion, and (3) the coating should be under compressive stress. In order to improve the coating adhesion as well as its bioactivity, certain research groups added HAp powder to bioactive glass to form a composite coating[11–13] and observed that nano-composites exhibit better mechanical properties compared to their micro counterparts.[14] These coatings generally obtained by plasma spray process are not chemically bonded with the underneath metallic substrates[11–12] and therefore interface are even otherwise weak and prone to separation under adverse loading conditions during initial insertion of implants. Although Gomez-vega et al. followed an enamelling technique[13] to obtain a better and more reliable coating-substrate bonding strength, detailed mechanical characterization under simulated conditions (during primary fixation of a load bearing orthopaedic implant) has not been reported so far. The success of bioactive glass coating on metallic implants especially Ti_6Al_4 V surface is not reported in literature.

In case of load bearing implants like orthopaedic and dental applications, the implant requires primary stability for subsequent osseointegration with the surrounding hard tissue. The

* Corresponding author. Tel.: +91 332473 3469; fax: +91 3324730957.
E-mail address: sdatta@cgcri.res.in (S. Datta).

0955-2219/$ – see front matter © 2009 Elsevier Ltd. All rights reserved.
doi:10.1016/j.jeurceramsoc.2009.02.013

process requires strong morphological fixation of the implant in the surrounding articulating bones. The coating surface are often scratched and abraded by surrounding articulating bones during the process. This degradation process of the coating can be best simulated with suitable scratch resistance testing process. Further, in long-term *in vivo* usage, continuous loading and unloading cycle for load bearing implants also causes continuous abrasion of the implant surface. This may results in coating failure and thereby leads to adverse reactions within the body and subsequently failure of the implant. It is well known that glass ceramic coatings possess much better set of mechanical properties compared to the parent glassy structure. A number of studies were reported incorporating different bioactive secondary phases mostly calcium phosphates to improve the mechanical properties of the resultant composites.[11–13,15] However, the majority of them are based on different bioactive polymers. There is little or no report on addition of secondary phase to any bioactive glass specially as coating. Only very recently, a report indicates that nano sized HAp (Nano-HAp) or fluoroapatite crystals improve the mechanical properties of resultant glass ionomer cement composites[15].

Further, it is mandatory to sterilize all artificial implants preferably with γ-ray with an approximate radiation dosage of 25 kGy.[16] This gamma irradiation is a clean, convenient, and effective method for sterilization of implant materials, which eliminates need for any special packaging. The effect of gamma irradiation on the biological properties of coating/interface has been studied in detail particularly on polymer-based materials.[17–20] However, very little studies have been reported on its effect on bioactive glass coating. Gamma irradiation being the strongest among all electromagnetic radiations may create some defects within silicate glasses[21–22] altering optical, mechanical and other structure related properties of the material. However there is no report on effect of Gamma radiation on any type of coating adhesion.

In the present study, a suitable bioactive glass containing B_2O_3 and TiO_2 was prepared and characterized. Composition of the glass system was tailored to match the thermal properties of the metallic substrates. Our earlier research on this glass composition established its biocompatibility and superior bone formation capability (Osseointegration) of porous scaffolds in Black Bengal Goat compared to HAp and β-tri Calcium Phosphate ceramics.[23–24] Bioactive glass and composite coating without and with HAp on Ti_6Al_4 V substrate was developed using a simple enamelling technique. Effect of HAp addition and gamma irradiation on the adhesion strength of the coating was evaluated by scratch resistance test and compared with that of pure bioactive glass coating.

2. Materials and methods

2.1. Preparation of bioactive glass powder

The preparation of this glass has been reported in our previous papers.[23–24] The oxide composition of the glass system is shown in Table 1

Table 1
Oxide composition range of bioactive glass, BG (mol%).

Components	SiO_2	Na_2O	CaO	P_2O_5	TiO_2	B_2O_3
BAG	57–60	9–11	21–24	2–3	0.5–1.5	2–3

2.2. Bioactive glass coating on Ti_6Al_4 V without and with HAp powder

Thick slurry of glass powder was prepared similarly using fine glass powder and the required amount of hydroxyapatite powder (10–25 wt% of the bioactive glass). Coating of bioactive glass was applied by normal enamelling technique on mechanically roughened and cleaned Ti_6Al_4 V substrates of flat coupons of size 20 mm × 20 mm × 2 mm and round small rod of diameter 2.0–5.0 mm (similar in dimension to small plugs for implantation in rabbit tibia and normal dental implants for dog and human subject). However, for characterization and evaluation of simple and composite bioactive glass coating small flat coupon samples were used. Same enamelling technique was followed to obtain a composite coating of bioactive glass-nano HAp on identical substrates. The nano sized HAp powder used for this work was prepared by solution-combustion,[25] method having a particle size in the range of 50–100 nm and agglomerated. The micro-HAp powder was produced by conventional co-precipitation and sintering process with a particle size range of 0.5–2.0 μm. The mixture of glass powder and HAp powder was further milled to result homogeneous slurry for application of uniform coating by spraying or dipping technique. The coated samples were thoroughly dried in an electric oven at 60 to 80 °C for overnight which were subsequently heat treated at 820 °C for 5 min (suitable for small coupons and rods) under reduced pressure using a dental furnace (VITA, VACUMET). The heat treatment schedule was established by analyzing a number of trials in the temperature range of 800–850 °C for different time which matches well with the firing schedule of other reported work in order to obtain defect free, adherent coating.[8]

2.3. Gamma irradiation of coated samples

Bioactive glass coated samples with and without HAp addition were irradiated with gamma ray from a ^{60}Co source at room temperature at a dose of 25 kGy with dose rate 9.54 kGy/h.

2.4. Structural characterization

Linear thermal expansion of the glass was measured using Orton Dilatometer-1600 D from room temp to 600 °C while room temperature XRD patterns of the coatings were recorded on a Philips (Philips Analytical, X'Pert, 1830, Netherlands) diffractometer in the 2θ range 20°–70° using CuKα ($\lambda = 1.54056$ nm) radiation for confirmation of the phases. The FTIR spectrum in the transmission mode of the bioactive glass sample was measured with a KBr pellet in a Varian 3600 FTIR spectrophotometer. For the spectra recorded in transmission, KBr pellets were prepared by mixing 1 mg of filtered powders

with ~50 mg of KBr in the spectral zone of 400–4000 cm^{-1}. Microstructure of the powders and coatings were studied using a SEM (LEO 430i, UK) along with quantitative EDX analysis using Si–Li detector to identify different area and phases in the microstructure. Adhesion of the coating was estimated by scratch testing of the coating using a Ducom Scratch Tester TR-01 attached with a load cell of 200 N and using a Rockwell diamond indenter. Scratch testing of the coated samples was carried out at an increasing load with loading rate 2.0–5.0 N/mm, scratch speed 0.1 mm/s and stroke length varying from 5–7 mm. Optical micrographs of the scratches were taken using an image analyzer (Correct, Seiwa Optical, Tokyo) for exact determination of the breaking load corresponding to the failure of the coating. For each coating type, samples ($n = 3$) were tested on three different well-separated positions. The average of all the data was taken as the breaking load. The impact strength of the bioactive glass coating was tested according to the IS: 3149–1994 specification by "falling ball" method, using a 1.0 kg ball with 10 cm dia. head. The other mechanical properties of the bioactive glass coating like hardness; fracture toughness etc. were measured by depth sensitive indentation technique (Fischerscope H100C XY_p, Fischer, Switzerland). The following equation was used for calculation of the "micro" scale fracture toughness[26–29]:

$$K_{ic} = \alpha\left(\frac{E}{H}\right)^{0.5}\left(\frac{P}{C^{1.5}}\right) \quad (1)$$

where, P is the applied load and C is the crack length measured from the centre of the Berkovich nanoindent and E and H are the Young's modulus and hardness of the coating, respectively, measured by the nanoindentation technique at the same applied load P at which K_{ic} of the coating is being measured. The α value was taken as 0.016.[27,28,30]

In vitro cytotoxicity test was performed on bioactive glass coated Ti_6Al_4 V samples. Both direct contact and test on extracts were performed as per ISO 10993-5, 1999 standard specification. The in vitro cytotoxicity test using direct contact method and test on extract method were performed using test samples, negative controls and positive controls. In direct method, all the specimens including negative control (Ultra High Molecular Weight Polyethylene) and positive control (PVC) were taken in triplicate and placed on subconfluent monolayer of L-929 mouse fibroblast cells using MEM supplemented with foetal bovine serum as the culture medium. After incubation of cells with test samples at 37 ± 2 °C for 24 ± 1 h, cell culture was examined microscopically for cellular response around test samples.

In test on extract method, the extract was prepared by incubating test materials with physiological saline at 37 ± 2 °C for 72 ± 2 h and made up with medium to get an extraction ratio of 1.25 cm^2/ml. 100% extracts were diluted to get concentrations of 50% and 25% with media. Different dilutions of extracts of test samples, negative controls (Ultra High Molecular Weight Polyethylene) and positive controls (Dilute phenol) in triplicate were placed on subconfluent monolayer of L-929 mouse fibroblast cells. After incubation of cells with extracts of test samples and controls at 37 ± 2 °C for 24 ± 1 h, cell cultures were examined microscopically for cellular response.

Cellular responses were scored as 0, 1, 2, and 3 according to non-cytotoxic, mildly cytotoxic, moderately cytotoxic and severely cytotoxic.

3. Results and discussion

The bioactive glass necessary to serve as a coating on different load bearing metallic implants (titanium and its alloy or stainless steel) should have matching thermal expansion coefficient in order to achieve a strong adhesion to the substrate. Further, to apply the coating by conventional vitreous enamelling technique the coating material should possess a softening temperature below the α → β transition temperature (955–1010 °C) of titanium.[31]

3.1. Selection of composition

The glass composition was formulated from Na_2O–CaO–SiO_2 glass system. Boric acid (H_3BO_3) and Titanium di-oxide was added to the composition in such a way that the thermal expansion coefficient (α) matched with that of the substrate (Ti_6Al_4 V alloy, $\alpha = 9.5–10.5 \times 10^{-6}$/°C at RT to 400 °C). Boric acid is widely used in manufacture of different commercial glasses usually to reduce the thermal expansion coefficient and softening temperature of the glass. Boric acid is antiseptic, antifungal, antibacterial also used in different medicine formulations used in the treatment of infection of ear, foot and wounds in humans and animals. Titanium di-oxide, a bio-inert oxide always found on bare metal implants, is used to improve chemical bonding between coating and substrate.

HAp, the main inorganic constituent of human bone, is widely used as a ceramic biomaterial, and added to the bioactive glass to increase the bioactivity of the composite coating and at the same time to reinforce the otherwise brittle glassy matrix. When dispersed in glass matrix, it formed a glass-ceramic that improved the mechanical properties of the coating. Since the mechanical properties of the glass ceramic materials is strongly dependent on particle size of the crystallites and increases with decreasing particle size, micro sized HAp powder and nano sized HAp powder [32–35] was used as a secondary phase in this case to study the effect of size of the second phase addition. In order to achieve a homogeneous microstructure in the resultant composite coating very fine glass particles (5–20 μm) are mixed thoroughly with HAp particles and applied as a coating by spraying or dipping.

Further, since object geometry plays a great role on adhesion property of the resultant coating in case of enamelling of glassy and glass-ceramic coatings, both flat coupons and round rod shaped objects (normal shape of actual implants) were used to ensure the suitability of the coating technology.

3.2. Cytotoxic evaluation

The bioactivity of the glass composition was tested before during the animal study with porous blocks where it was found to be more osseoinductive compared to hydroxyapatite and

Table 2
Mechanical properties of the bioactive glass.

Glass code	Load (Kg)	Young's modulus (GPa)	Vicker's hardness (GPa)	Fracture toughness (MPa-m$^{1/2}$)
BAG	1.0	72.0	6.52	0.74

β-tri-calcium phosphate.[23,24] However, the bioactive glass coating was not tested. The cytotoxicity test of the coating by direct contact and test on extract method indicates non-cytotoxic behaviour of the bioactive glass coating as shown in Fig. 1a and b. Cellular response as measured by the scale was 0 indicating non-cytotoxic behaviour. Negative control gave non-cytotoxic response and positive control gave severely cytotoxic response as expected.

3.3. Structural characterization

The glass softening temperature was found to be <750 °C from DTA results which help preventing excessive oxidation of the alloy during enamelling. The linear coefficient of thermal expansion (α) of the glass was measured to be 10.93×10^{-6}/°C

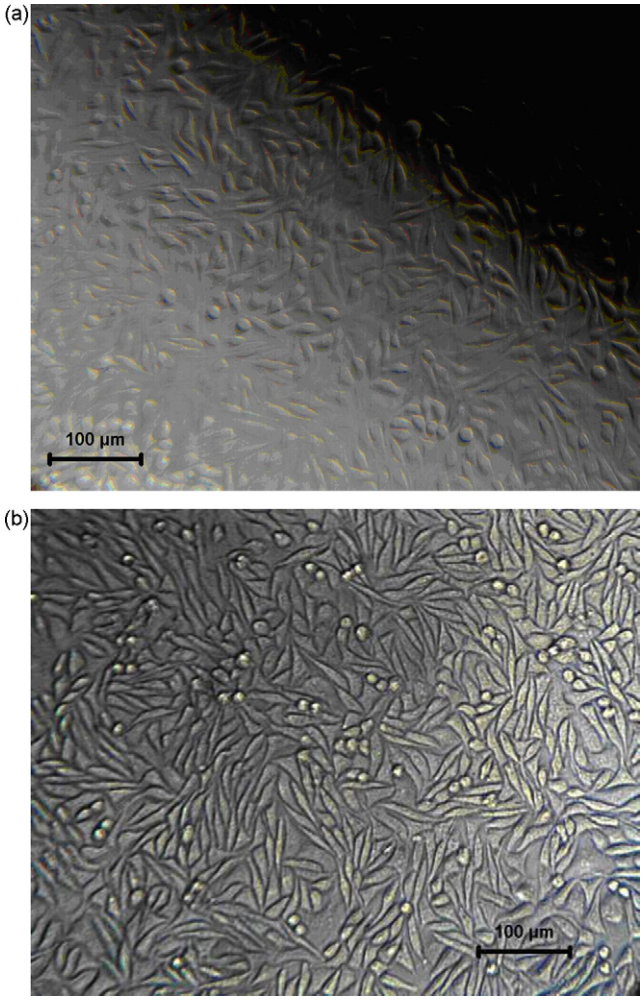

Fig. 1. Cellular response after Cytotoxicity test on bioactive glass. (a) by direct contact method, (b) by extract method.

at RT to 600 °C, which is very much comparable with that of the base metal.

The XRD analysis showed the glass and the resultant coating to be amorphous in nature. After heat treatment at 650 °C for 1 h, some crystallites formed with peaks corresponding to quartz and $Na_2Ca_2Si_3O_9$ crystalline phases.

The FT-IR spectra (Fig. 2) shows two broad strong absorption bands at ~1050 cm^{-1} and 480 cm^{-1} which can be assigned to Si–O and P–O vibrations, respectively. B–O stretching of BO_3 units may be assigned to the weak broad band at 1300–1450 cm^{-1}.[32] However, the existence of different groups like borate and phosphates can not be pin pointed accurately because of super imposition of different peaks.

Mechanical properties of the glass coating showed in Table 2. The hardness and the Young's Modulus values are superior compared to other bioactive glass coating compositions already reported by other researchers.[13]

SEM micrographs of the nano HAp powder used is shown in Fig. 3. As observed, the particle size was measured to be in the range of 50–100 nm. Prolonged wet milling of powdered bioactive glass and other fine-grained ingredients of comparable density in a planetary ball mill ensures a uniform mixing of all the components in the resultant composite slurry.

In vitreous enamelling technique the thickness of the applied glassy or composite coating is easily controllable with a good degree of accuracy and in many industrial applications this process has been automated. Coating thickness can be controlled by controlling some of the process parameters like rheological properties of the coating material slurry which is applied on the metal and also by controlling the green coating thickness and number of applications. The coating thickness obtained on the surface of Ti_6Al_4V (as in case of dental implants) was about ~80 µm, it is almost uniform over the surface and the interface is rough and relatively thick (~4.0 µm) indicating strong chemical bonding (Fig. 4). The small defects present in the

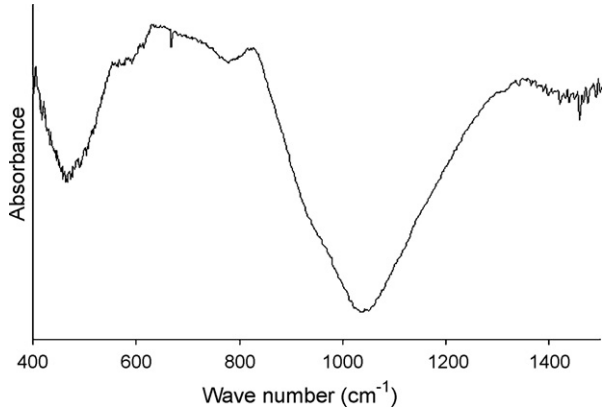

Fig. 2. FTIR spectrum of bioactive glass powder.

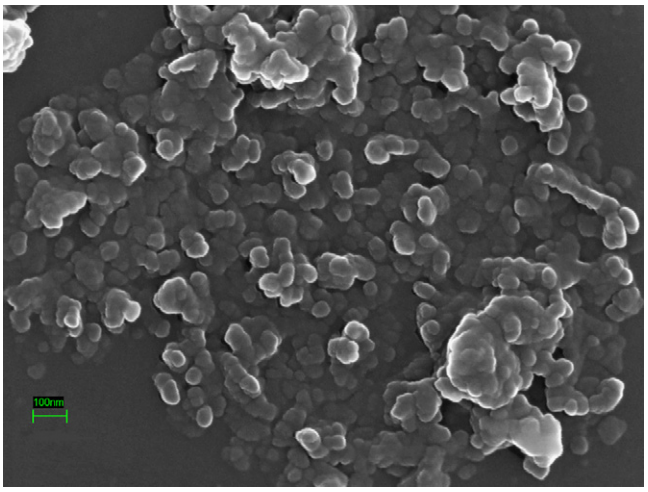

Fig. 3. SEM micrograph of nano-HAp powder.

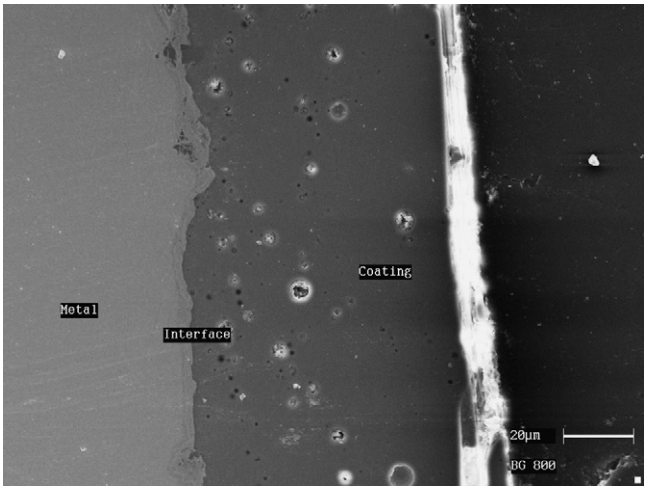

Fig. 4. SEM micrograph of cross section of BG coating on Ti-6Al4 V.

coating metal interface, are some trapped gas bubble which normally occurs in case of titanium and its alloy enamelling as reported by other authors.[31] The thickness of the coating metal interface (∼4.0 μm) is indications of the extent of inter

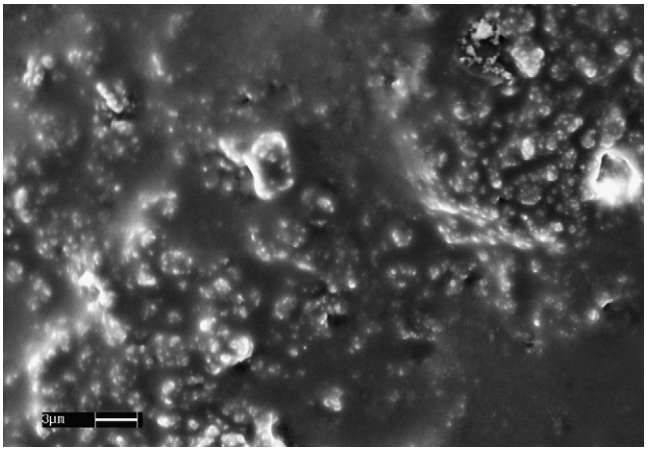

Fig. 5. SEM micrograph of BG-micro HAp composite coating.

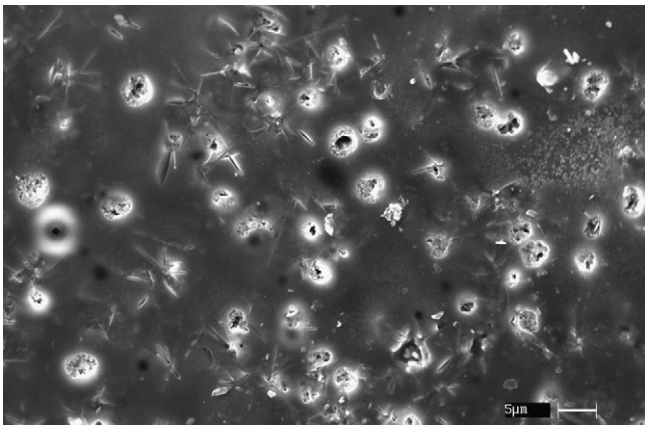

Fig. 6. SEM micrograph of BG-nano HAp composite coating.

diffusion of resulting low valent metal oxide in the molten glass matrix which indirectly quantifies the chemical bonding as reported in the literature. The mechanism of bonding of silicate glasses with titanium and its alloys has already been reported in the literature.[36–37] This was corroborated by measuring impact strength of the glassy coating by "Falling Ball"

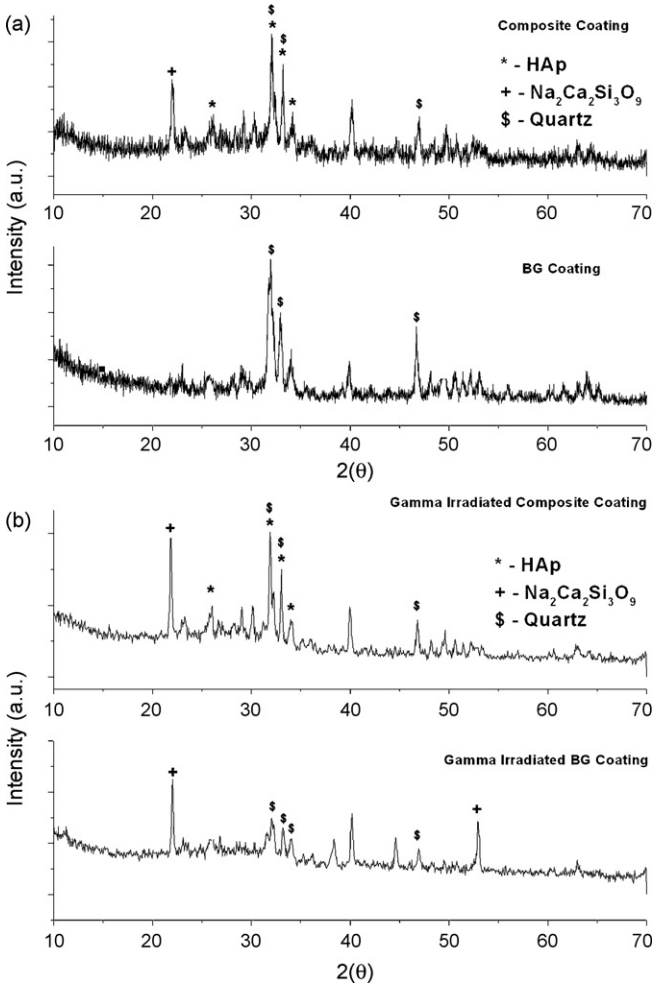

Fig. 7. XRD patterns of BG coating and Composite coating (a) before and (b) after gamma irradiation.

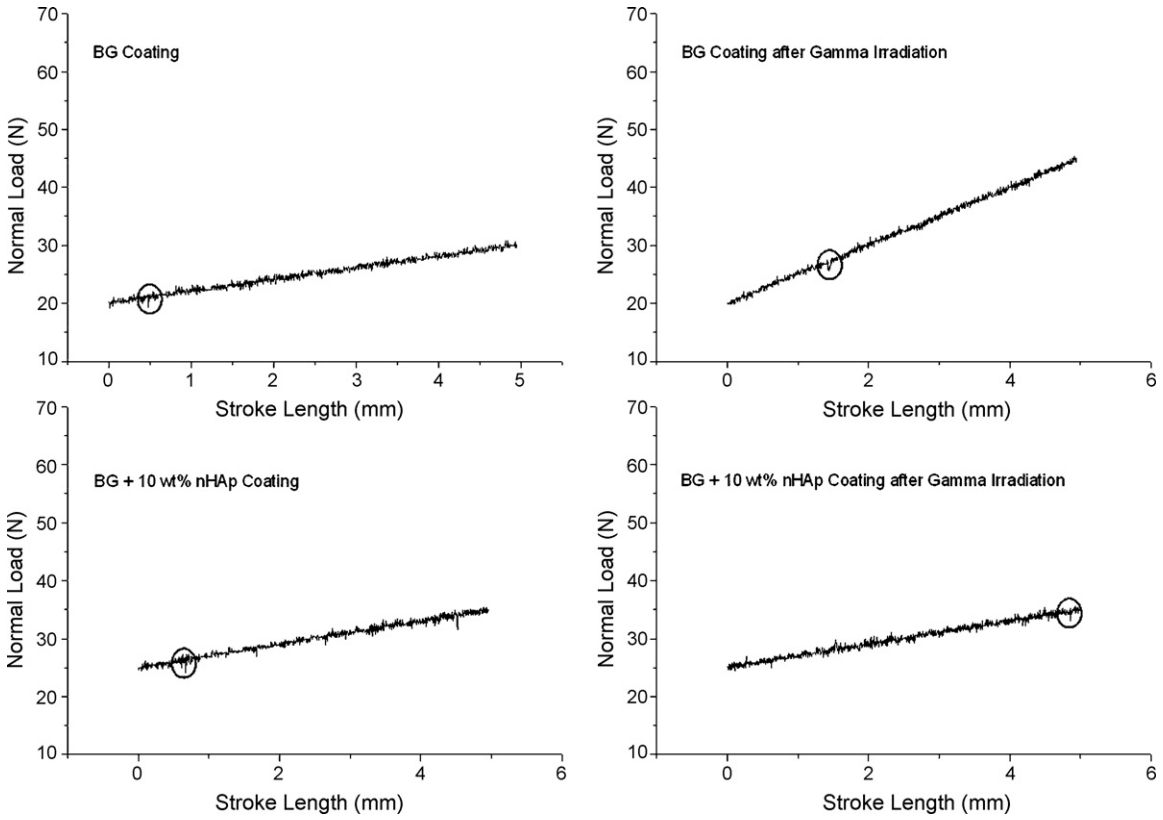

Fig. 8. Load displacement curve of BG coating and composite coating before and after gamma irradiation (circled portion showing the breaking load).

method, which indicates the coating has impact strength of more than 40KN, a value much better than conventional glassy coatings on mild steel substrates applied by vitreous enamelling process.[38] Micrograph of micro-HAp composite coating showed dispersion of nearly spherical HAp particles (sometimes agglomerated) in the glassy matrix (Fig. 5). In case of nano-HAp dispersed composite bioactive glass coatings the micrograph (Fig. 6) showed similar uniform distribution of agglomerated HAp particles throughout the coating matrix. In addition, small needle like crystals (almost whiskers) of HAp (1.0–5.0 μm) appeared surrounding some nano HAp particles in the matrix. The composition of different phases or components in the micrograph was ascertained with quantitative EDX analysis. Fig. 7a shows the XRD spectra of bioactive glass and bioactive glass–nano HAp composite coatings. After heat treatment, peaks corresponding to quartz and $Na_2Ca_2Si_3O_9$ crystalline phases were obtained in case of only bioactive glass coating where as some HAp peaks were found to coexist along with the above phases in composite coating. The effect of γ-sterilization on the XRD-patterns of these coatings is quite significant. Though hardly any change was observed in case of HAp peaks, in the composite coating, a significant increase in peak intensity occurred in case of quartz and $Na_2Ca_2Si_3O_9$ phases, implying an increase in volume fraction of these phases after gamma irradiation (Fig. 7b) in both bioactive glass (BAG) and composite coatings. In case of BAG coating, intensity of quartz peak increased from 50% to 78.2% and that of $Na_2Ca_2Si_3O_9$ phase from 30% to 83%. The exact reason or mechanism of this selective change in microstructure in bioactive glass coating by γ-ray exposure is not clear. However, this type of behaviour is not unexpected, and many apparently contradictory results for different silicate based glass systems were reported earlier by other investigators.[39–42]

The scratch test is a standard technique to measure the coating/substrate adhesion.[43–50] Scratch testing consists of introducing stresses at the interface between the coating and the substrate. This is achieved by pressing a diamond stylus on the sample surface with a normal load. Many different modes of failure are observed which include coating detachment, through-thickness cracking and plastic deformation or cracking in the coating, interface or substrate.[51–54] In fact, it is usual that several different failure modes occur at the same time and this can make the results of the test difficult to interpret. The critical load for adhesion failure is easiest to identify in the case of a hard, relatively brittle film on a softer substrate.

In case of hard and brittle bioactive glass coating on compliant metallic substrate of Ti_6Al_4 V alloy, three different types of failure mode can operate simultaneously, (i) through-thickness cracking, (ii) coating detachment and (iii) chipping within the coating.

From the results shown in Fig. 8(a), it was observed that the critical load (adhesion strength) for only BAG coating was lower (21 N) than that of the micro-HAp composite (10 wt%) glass ceramic coating (27 N) and nano-HAp composite (15 wt%) glass ceramic coating (32 N). However, it is observed that addition of more than 10 wt% of micro HAp powder and 15 wt% of nano HAp powder did not make any impact on adhesion strength of the resultant composite coating. An enhancement in adhesion

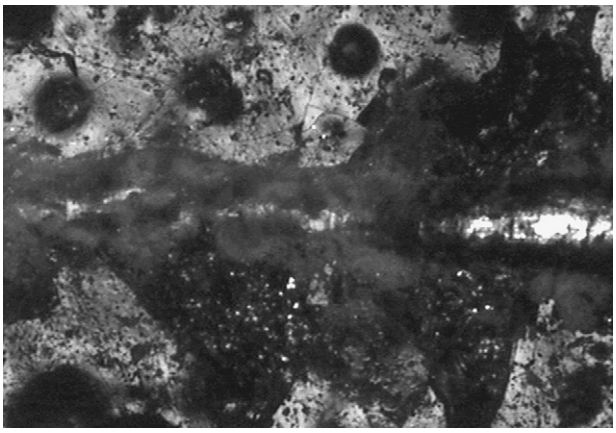

Fig. 9. Optical micrographs of the scratches of BG coating.

strength of the coatings was observed when they were irradiated under gamma ray at 25 kGy. As a result, a 28 N breaking load was required for gamma irradiated bioactive glass coating and 38 N for nano HAp composite coating. Graphs of the respective scratches are shown in Fig. 8(b). Figs. 9–12 show the optical micrographs of scratch tested samples particularly highlighting the coating failure area. With increasing load, all the coating failed by chipping off from the metal substrate. When seen under image analyzer, fine cracks (originating from the indentation site and moving across the glassy coating away in all direction) were found to be present in case of only BAG coating (Fig. 9), a characteristic feature of glass coating, where as they were totally absent in composite coatings (Fig. 10). The glassy coating fractured as the normal load was increased by coming out as flakes. In case of composite coatings, the scratch patterns were more or less smooth with regular material removal along the scratch path. Some small cracks were observed in the scratch path, which moves perpendicular to scratch direction which fails to penetrate the composite matrix. More coating delamination was observed in case of non-irradiated glassy coating compared to the gamma irradiated one (Figs. 11 and 12). Optical micrographs of scratch tested sample shows brittle nature of bioactive glass coating where coating flakes out with increasing load. In case of composite coating, the scratch pattern is uniform

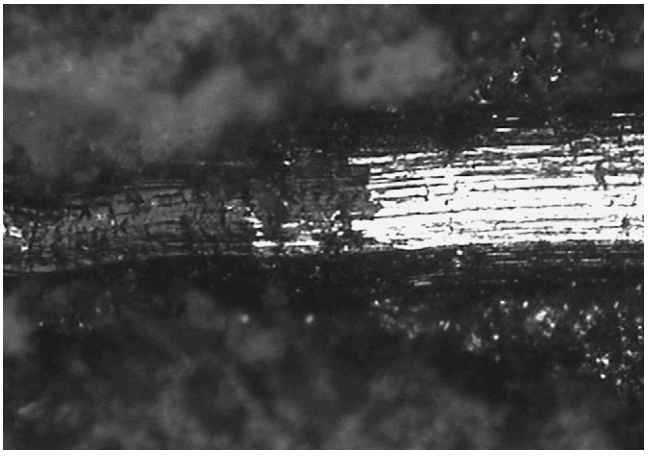

Fig. 10. Optical micrographs of the scratches of Composite coating.

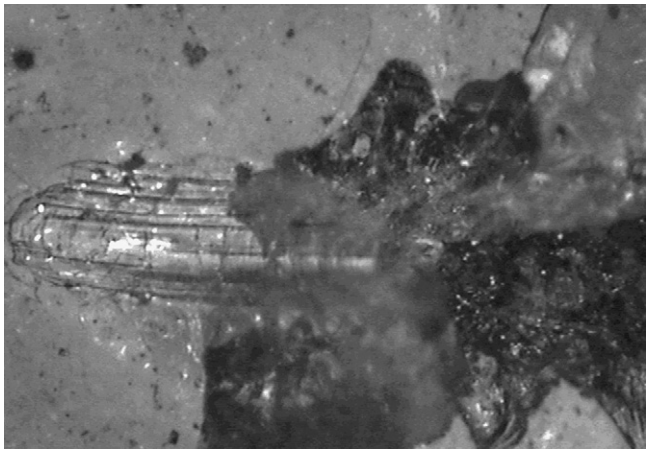

Fig. 11. Optical micrographs of the scratches of gamma irradiated BG coating.

and no flaking of material occurred with increase in applied load.

In general, propagation of cracks in glassy coating occurs due to the uneven stress distribution generated by a mismatch in thermal expansion coefficient between the substrate and coating and rapid thermal quenching during coating processing, as a result, chipping within the bioactive glass coating and through thickness delamination was observed. Addition of nano-sized HAp particles to glassy coating changes the stress distribution pattern in the glass-ceramic matrix, which in turn reduce the possibilities of crack propagation process and eliminate through-thickness cracking and chipping within the glass-ceramic coating.[55] During scratch test, grain boundaries of the dispersed HAp phase restricted crack propagation in the matrix by crack deflection reducing chances for catastrophic failure, which resulted improvement of strength of the coating. On the other hand, in case of only BAG coating, numerous fine cracks originated from the scratch and catastrophic failure occurred due to unhindered crack propagation leading to low coating adhesion strength. The adhesion strength of the coating (Bioactive glass and composite) theoretically depends on the strength of the chemical bond between the coating and the substrate through the interface and therefore, it should have been almost same in all the composite

Fig. 12. Optical micrographs of the scratches of gamma irradiated Composite coating.

coatings with same base glass. But the mechanism of failure in scratch tests for different composite coatings is so different that the experimental breaking load of different types of coatings differs to a great extent.

Exposure to γ-irradiation improves scratch resistance of bioactive glass and composite coatings and improves crystallization of bioactive glass coatings resulting in a glass ceramic material (with different distribution of phases) having better set of mechanical properties. The strong and deep penetrating γ-rays can cause microstructural change[20,22] as shown by XRD analysis in the bulk coating (only 150 μm thick), possibly by creating defects and is likely to affect the coating-metal interface and increase the adherence as reflected in the scratch test results.

4. Conclusions

A novel bioactive glass composition using B_2O_3 and TiO_2 was developed by conventional glass melting technique and characterized to establish its structure and properties. The bioactive glass and the composite coating developed is suitable for application as coating on titanium based and stainless steel alloys used for load bearing implant fabrication. The composite coating exhibits significantly improved scratch resistance property, which are expected to resist the scratching due to friction with the surrounding hard tissues during initial insertion of the implant and can improve the performance of the coated implants in achieving better primary strength during cementless fixation. 10 wt% micro HAp and 15 wt% nano HAp can be used to improve the adhesion strength of the resultant composite coating.

Sterilization using γ-irradiation improves scratch resistance of both bioactive glass and composite coatings and improves crystallization of bioactive glass coating resulting in a different glass ceramic material having better set of mechanical properties.

The mechanism by which strengthening of bioactive glass coating takes place due to γ-sterilization is not well understood.

Acknowledgement

The authors are obliged to Dr B.N. Mondal of CMERI, Durgapur, India for providing the facility to use the scratch tester and image analyzer. They are also grateful to Dr. S. Sen for SEM micrographs and Dr. B. Mukherjee of Refractory Division for α measurement. Finally, sincere thanks are due to Dr. H.S. Maiti, Director for his kind interest in this work and DST, India for the funding.

References

1. Yan, W. Q. and Davies, J. E., Bone formation around surface modified titanium implants. *Bioceramics*, 1998, **11**, 659–662.
2. Nishiguchi, S., Nakamura, T., Kobayashi, M., Miyagi, F. and Kokubo, T., The effect of heat treatment on bone bonding ability of alkali-treated titanium. *Biomaterials*, 1999, **20**, 491–500.
3. Cook, S. D., Thomas, K. A. and Jarcho, M., Hydroxyapatite coated porous titanium for use as an orthopaedic biologic attachment system. *Clin. Orthop. Relat. Res.*, 1988, **230**, 303–312.
4. Geesink, R. G. T., Hydroxyapatite coated hip implants. Ph.D. Thesis, Rijksuniversiteit Limburg te Maastricht; 1998.
5. Hench, L. L. and Anderson, O., Bioactive glass coatings. In *An Introduction to Bioceramics*, ed. L. L. Hench and J. Wilson. World Scientific, Singapore, 1993, pp. 239–259.
6. Pazo, A., Saiz, E. and Tomsia, A. P., Silicate glass coatings on Ti-based implants. *Acta. Mater.*, 1998, **46**, 2551–2558.
7. Pazo, A., Saiz, E. and Tomsia, A. P., Bioactive coatings on Ti and Ti_6Al_4 V alloys of medical applications. In *Ceramic Microstructures*, ed. A. P. Tomsia and A. M. Glaeser. Plenum Press, New York, 1998, pp. 543–550.
8. Gomez-Vega, J. M., Saiz, E. and Tomsia, A. P., Glass-based coatings for titanium implant alloys. *J. Biomed. Mater. Res.*, 1999, **46**, 549–559.
9. Soundrapandian, C., Datta, S. and Sa, B., Drug eluting implants for osteomyelitis. *Crit. Rev. Therap. Drug Carrier Sys.*, 2007, **24**, 493–545.
10. Hench, L. L., Bioceramics: from concept to clinic. *J. Am. Ceram. Soc.*, 1991, **74**, 1487–1510.
11. Carvalho, F. L. S., Borges, C. S., Branco, J. R. T. and Pereira, M. M., Structural analysis of hydroxyapatite/bioactive glass composite coatings obtained be plasma spray processing. *J. Non-Cryst. Sol.*, 1999, **247**, 64–68.
12. Lin, J. H. C., Liu, M. L. and Ju, C. P., Structure and properties of hydroxyapatite-bioactive glass composites plasma sprayed on Ti_6Al_4 V. *J. Mater. Sci: Mater. Med.*, 1994, **5**, 279–283.
13. Gomez-Vega, J. M., Saiz, E., Tomsia, A. P., Marshall, G. W. and Marshall, S. W., Bioactive glass coatings with hydroxyapatite and bioglass particles on Ti-based implants. 1. *Processing Biomater.*, 2000, **21**, 105–111.
14. Esteban, S. L., Suarez, T. R., Betegón, F. E., Pecharromán, C. and Moya, J. S., Mechanical properties and interfaces of zirconia/nickel in micro- and nanocomposites. *J. Mater. Sci.*, 2006, **41**, 5194–5199.
15. Moshaverinia, A., Ansari, S., Moshaverinia, M., Roohpour, N., Darr, J. A. and Rehman, I., Effects of incorporation of hydroxyapatite and fluoroapatite nanobioceramics into conventional glass ionomer cements (GIC). *Acta Biomat.*, 2008, **4**, 432–440.
16. ISO Designation (1138/1, 1137), Radiation sterilization of health care products using gamma rays.
17. Suwanprateeb, J., Tanner, K. E., Turner, S. and Bonfield, W., Influence of sterilization by gamma irradiation and of thermal annealing on creep of hydroxyapatite-reinforced polyethylene composites. *J. Biomed. Mater. Res.*, 1998, **39**, 16–22.
18. Nuutinen, J. P., Välimaa, T., Clerc, C. and Törmälä, P., Mechanical properties and in vitro degradation of bioresorbable knitted stents. *J. Biomat. Sci.*, 2002, **13**, 1313–1323.
19. Kurtz, S. M., Rimnac, C. M., Hozack, W. J., Turner, J., Marcolongo, M., Goldberg, V. M., Kraay, M. J. and Edidin, A. A., In vivo degradation of polyethylene liners after gamma sterilization in air. *J. Bone Joint Surg. Am.*, 2005, **87**, 815–823.
20. An, Y. H., Alvi, F. I., Kang, Q., Laberge, M., Drews, M. J., Zhang, J., Matthews, M. A. and Arciola, C. R., Effects of sterilization on implant mechanical property and biocompatibility. *Int. J. Artif. Organs.*, 2005, **28**, 1126–1137.
21. Griscom, D. L., Optical properties and structural defects in silica glass. *Ceram. Soc. Jpn.*, 1991, **99**, 923–942.
22. Kundu, D., Patra, A. and Ganguli, D., Study of γ–radiation induced defects in fumed silica-alkoxide derived silica glasses. *J. Mater. Sci. Lett.*, 2000, **19**, 37–39.
23. Ghosh, S. K., Nandi, S. K., Kundu, B., Datta, S., De, D. K., Roy, S. K. and Basu, D., Interfacial response of hydroxyapatite and tri-calcium phosphate prepared by a novel aqueous combustion method: A comparison with bioglass *in vivo* implanted in goat. *J. Biomed. Mat. Res.*, 2008, **86B**, 217–227.
24. Nandi, S. K., Kundu, B., Datta, S., De, D. K. and Basu, D., The repair of segmental bone defects with porous bioglass: An experimental study in goat. *Res. Vet. Sci.*, 2009, **86**, 162–173.
25. Ghosh, S. K., Datta, S. and Roy, S. K., Solution combustion synthesis of Calcium hydroxyapatite nanoparticles. *Trans. Ind. Cer. Soc.*, 2004, **63**, 27–32.
26. Evans, A. G., Lawn, B. R. and Marshall, D. B., Elastic/plastic indentation damage in ceramics: the median/radial crack system. *J. Am. Ceram. Soc.*, 1980, **63**, 574–581.

27. Dukino, D. R. and Swain, M. V., Comparative measurement of fracture toughness with berkovich and vickers indenters. *J. Am. Ceram. Soc.*, 1992, **75**, 3299–3304.
28. Chen, J. and Bull, S. J., Assessment of the toughness of thin coatings using nanoindentation under displacement control. *Thin Solid Films*, 2006, **494**, 1–7.
29. Mullins, L. P., Bruzzi, M. S. and McHugh, P. E., Measurement of the microstructural fracture toughness of cortical bone using indentation fracture. *J. Biomech.*, 2007, **2007**(40), 3285–3288.
30. Shikimaka, O. and Grabco, D., Deformation created by Berkovich and Vickers indenters and its influence on surface morphology of indentations for LiF and CaF_2 single crystals. *J. Phys. D: Appl. Phys.*, 2008, **41**, 1–6.
31. Lopez-Esteban, S., Saiz, E., Fujino, S., Oku, T., Suganuma, K. and Tomsia, A. P., Bioactive glass coatings for orthopedic metallic implants. *J. Eur. Ceram. Soc.*, 2003, **23**, 2921–2930.
32. Agathopoulos, S., Tulyaganov, D. U., Ventura, J. M. G., Kannan, S., Karakassides, M. A. and Ferriera, J. M. F., Formation of hydroxyapatite onto glasses of the CaO-MgO-SiO_2 system with B_2O_3, Na_2O, CaF_2 and P_2O_5 additives. *Biomaterials*, 2006, **27**, 1832–1840.
33. Kingsley, J. J. and Patil, K. C., A novel combustion process for the synthesis of fine particle α-alumina and related oxide materials. *Mater. Lett.*, 1988, **6**, 427–432.
34. Ye, T., Guiwen, Z., Weiping, Z. and Shangda, X., Combustion synthesis and photoluminescence of nanocrystallineY_2O_3:Eu phosphors. *Mater. Res. Bull.*, 1997, **32**, 501–506.
35. Tas, A. C., Combustion synthesis of calcium phosphate bioceramic powders. *J. Eur. Ceram. Soc.*, 2000, **20**, 2389–2394.
36. Donald, I. W., Preparation, properties and chemistry of glass- and glass-ceramic-to-metal seal and coatings. *J. Mater. Sci.*, 1993, **28**, 2841–2886.
37. J. Schrooten and J. A. Helsen, Adhesion of bioactive glass coating to Ti_6Al_4 V oral implant. Biomaterials, **21**(14).
38. Datta, S., Studies on broad spectrum corrosion resistant oxide coatings. *Bull. Mater. Sci.*, 2001, **24**, 569–577.
39. Zdaniewski, W. A., Easler, T. E. and Bradt, R. C., Gamma radiation effects on the strength of a borosilicate glass. *J. Am. Ceram. Soc.*, 1983, **66**, 311–313.
40. Swift, R., Effect of gamma radiation on the strength of plate glass of varying arsenic content. *J. Am. Ceram. Soc.*, 1981, **64**, 145–146.
41. Doweidar, H., Zeid, M. A. A. and El-Damrawy, G. M., Effect of gamma radiation and thermal treatment on some physical properties of ZnO-PbO-B_2O_3 glasses. *J. Phys. D: Appl. Phys.*, 1991, **24**, 2222–2228.
42. Badr, Y., El'Khoudary, M. A. and Annan, I., Evaluation of some properties of dental ceramic as affected by different types of lasers and gamma radiations. In *Lasers in Dentistry X, Proceedings of SPIE*, ed. P. Rechmann, D. Fried and T. Hennig, 2004, pp. 72–90.
43. Perry, A. J., The adhesion of chemically vapour deposited hard coatings to steel—the scratch test. *Thin Solid Films*, 1981, **78**, 77–93.
44. Bull, S. J. and Berasetegui, E. G., An overview of the potential of quantitative coating adhesion measurement by scratch testing. *Tribol. Int.*, 2006, **39**, 99–104.
45. Forsgren, J., Svahn, F., Jarmar, T. and Engqvist, H., Formation and adhesion of biomimetic hydroxyapatite deposited on titanium substrates. *Acta Biomater.*, 2007, **3**, 980–984.
46. Perry, A. J., Scratch adhesion testing of hard coatings. *Thin Solid Films*, 1983, **107**, 167–180.
47. Hintermann, H. E., Adhesion, friction and wear of thin hard coatings. Wear, **100**, 381–397.
48. Steinmann, P. A. and Hintermann, H. E., Adhesion of TiC and TiCN coatings on steel. *J. Vac. Sci. Technol.*, 1985, **A3**, 2394–2400.
49. Valli, J., A review of adhesion test methods for thin hard coatings. *J. Vac. Sci. Technol.*, 1986, **A4**, 3001–3014.
50. Bull, S. J. and Rickerby, D. S., New developments in the modelling of the hardness and scratch adhesion of thin films. Surf. Coat. Technol., **42**, 149–164.
51. Benjamin, P. and Weaver, C., Measurement of adhesion of thin films. *Proc. Roy. Soc. Lond., Ser. A.*, 1960, **254**, 163–176.
52. Bull, S. J., Failure modes in scratch adhesion testing. *Surf. Coat. Technol.*, 1991, **50**, 25–32.
53. Bull, S. J., Spallation failure maps from scratch testing. *Mater. High Temp.*, 1995, **13**, 169–174.
54. Bull, S. J., Failure mode maps in the thin film scratch adhesion test. *Tribol Int.*, 1997, **30**, 491–498.
55. Xu, C., Effects of particle size and matrix grain size and volume fraction of particles on the toughening of ceramic composite by thermal residual stress. *Ceram. Int.*, 2005, **31**, 537–542.